Eye–Hand Coordination during Reaching. II. An Analysis of the Relationships between Visuomanual Signals in Parietal Cortex and Parieto-frontal Association Projections

Alexandra Battaglia-Mayer[1,2], Stefano Ferraina[1], Aldo Genovesio[1], Barbara Marconi[1], Salvatore Squatrito[3], Marco Molinari[2], Francesco Lacquaniti[2,4] and Roberto Caminiti[1,5]

[1]Dipartimento di Fisiologia umana e Farmacologia, Università di Roma 'la Sapienza', piazzale Aldo Moro 5, 00185 Rome, [2]IRCCS Santa Lucia, via Ardeatina 306, 00179 Rome, [3]Dipartimento di Fisiologia umana e generale, Università di Bologna, Piazza di Porta S. Donato 2, 40127 Bologna, [4]Dipartimento di Neuroscienze, Università di Roma 'Tor Vergata', 00179 Rome, Italy and [5]INSERM U. 483, Université Pierre et Marie Curie, 9 quai St Bernard, 75005 Paris, France

The relationships between the distribution of visuomanual signals in parietal cortex and that of parieto-frontal projections are the subject of the present study. Single cell recording was performed in areas PEc and V6A, where different anatomical tracers were also injected. The monkeys performed a variety of behavioral tasks, aimed at studying the visual and motor properties of parietal cells, as well as the potential combination of retinal-, eye- and hand-related signals on cell activity. The activity of most cells was related to the direction of movement and the active position of the hand. Many of these reach-related cells were influenced by eye position information. Fewer cells displayed relationships to saccadic eye movements. The activity of most neurons related to a combination of both hand and eye signals. Many cells were also modulated during preparation for hand movement. Light–dark differences of activity were common and interpreted as related to the sight and monitoring of hand motion and/or position in the visual field. Most cells studied were very sensitive to moving visual stimuli and also responded to optic flow stimulation. Visual receptive fields were generally large and extended to the periphery of the visual field. For most neurons, the orientation of the preferred directions computed across different epochs and tasks conditions clustered within a limited sector of space, the field of global tuning. This can be regarded as an ideal frame to combine spatially congruent eye- and hand-related information for different forms of visuomanual behavior. All these properties were common to both PEc and V6A. Retinal, eye- and hand-related activity types, as well as parieto-frontal association cells, were distributed in a periodic fashion across the tangential domain of areas PEc and V6A. These functional and anatomical distributions were characterized and compared through a spectral and coherency analysis, which revealed the existence of a selective 'match' between activity types and parieto-frontal connections. This match depended on where each individual efferent projection was addressed. The results of the present and of the companion study can be relevant for a re-interpretation of optic ataxia as the consequence of the breakdown of the combination of retinal-, eye- and hand-related directional signals within the global tuning fields of parietal neurons.

Introduction

Areas PEc [parietal area PEc; area 5 (part)] and V6A [visual area 6A, area 19 (part)] are parts of posterior parietal cortex. Recent studies (Galletti *et al.*, 1997; Johnson *et al*, 1997; Battaglia Mayer *et al.*, 1998; 2000; Caminiti *et al.*, 1998, 1999) have assigned to V6A a visuomotor role during reaching. Preliminary information (Ferraina *et al.*, 2001; Squatrito *et al.*, 2001) indicates that PEc is involved in visual processing and motor functions.

As part of area 5, PEc should be regarded as a somatosensory 'association' cortex (Critchley, 1953). However, no representation of the somatosensory periphery has ever been described in this part of the superior parietal lobule. The results of the accompanying anatomical study have shown that PEc receives local projections from a variety of visuomotor parietal areas and entertains privileged relationships with dorso-caudal premotor cortex, in the frontal lobe (Marconi *et al.*, 2001). This frontal region is rich in neurons related to hand movement direction and active position in space (Caminiti *et al.*, 1991; Wise *et al.*, 1997; Fujii *et al.*, 2000). Furthermore, dorso-caudal premotor cortex is a main source of cortico-cortical input to motor cortex.

These anatomical relationships suggest a visuomotor role for PEc and for the information conveyed by its projections to the frontal cortex. For these reasons, behavioral neurophysiology was adopted to characterize the functional properties of neurons in this part of the parietal lobe.

The behavioral tasks used were aimed at assessing the influence of retinal-, eye- and hand-related signals on parietal cell activity, under a variety of experimental conditions. These required different forms of eye–hand coordination, such as those necessary for reaching to foveated and to extrafoveal targets within a typical reaction-time paradigm, or after a delay interval, with prior knowledge of target location, or, finally, to make saccade to visual targets, without subsequent hand movement. Across these tasks, some forms of visuo-manual behavior were repeated under different conditions. This allowed the evaluation of the context dependency of parietal cell activity.

As a final step, we have investigated whether these signals had access to the cortico-cortical efferent system projecting to the frontal lobe. To this aim, the distribution of functional properties in the parietal cortex was contrasted with that of the parieto-frontal association cells described in the companion paper (Marconi *et al.*, 2001).

Materials and Methods

Animals

Three hemispheres of two rhesus monkeys (*Macaca mulatta*; body weights 3.7 and 3.5 kg) were used in this study. Monkeys (NI and ME) were the same animals used for the anatomical experiments [see Table 1 of the companion paper (Marconi *et al.*, 2001)]. Recordings were made in one hemisphere of NI and in both hemispheres of ME.

Behavioral Tasks

Extracellular single cell recording was made in areas V6A and PEc while the animals performed six different behavioral tasks. The monkeys sat on a primate chair, with their eyes 17 cm in front of a touch-sensitive (MicroTouch Systems, Wilmington, DE, USA) computer monitor used to display the tasks and control the animals' hand position. Eye position was controlled by using implanted scleral search coils (1° resolution) and sampled at 100 Hz (Remmel Labs, Ashland, MA, USA). Fixation accuracy was controlled through circular windows (3.5°) around the targets. Hand position and accuracy were controlled on the touch screen through 3 cm diameter circular windows (10° visual angle).

In the four reaching tasks and in the saccade task, the hand and/or the eye moved from a central positions to eight different targets, randomly

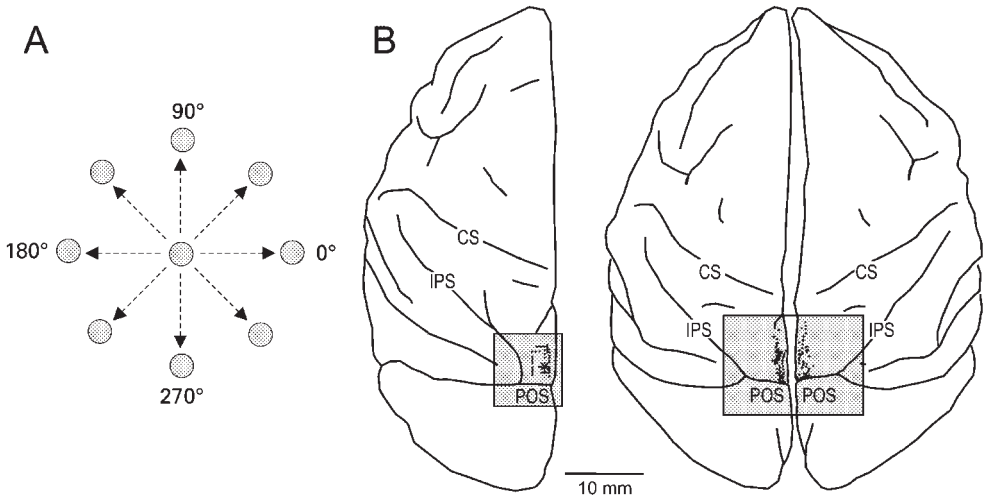

Figure 1. (*A*) Directional layout of the workspace where the behavioral tasks were performed. The arrows indicate the direction of eye and/or hand movement, the circles indicate the positions of the central and peripheral targets. (*B*) Brain figurines with microelectrode penetrations. Dorsal views of the left hemisphere of monkey NI (left) and of both hemispheres of monkey ME (right), with entry points (dots) of microelectrode penetrations in area PEc. POS, IPS and CS indicate parieto-occipital, intraparietal and central sulci, respectively.

selected at 45° angular intervals on a virtual circle with radius subtending 24° visual angle (Fig. 1*A*). These tasks were (i) a conventional hand Reach task (R), where eye and hand movements to visual targets were made within a reaction-time paradigm; (ii) a Reach-Fixation task (RF), where hand movements were made in absence of eye movement, with eye position kept constant at the center of the workspace; (iii) a Saccade task (S), where eye movements were made from a common central origin to eight different targets, the same used for the reaching tasks; during this task, time constraints (50 and 500 ms, lower and upper limits) were made on reaction time of saccades, the hand position was fixed and was controlled through a telegraph key; (iv–v) in the Instructed-Delay Reach task (IDR), the animals fixated and touched a red center stimulus for a variable control time. Then, one of eight green targets was lit, as instruction signal for the next hand movement. After a variable reaction time (D_1; 300 ms, upper limit) and movement time (D_2), the eye achieved the green target and stayed there for the remainder (D_3) of the instructed-delay time (IDT; 1–2.5 s) and during the upcoming hand movement and static holding on the target. During the entire IDT the animal was required to withhold the hand movement until the green light was turned red. This was the go signal for the hand to reach toward the target and to stay there for a variable target holding time. The duration of D_1 and D_2 was determined in off-line analyses. This task was performed in normal light conditions (l) and in total darkness (d) to evaluate the influence of the visual feedback of hand movement and position on cell activity; and (vi) a Visual Fixation task (VF), where visual stimuli were presented and moved in the visual field while the animal kept constant fixation at the center of the workspace. The stimuli used were: (i) conventional solid bars moving across the screen, in order to map the visual receptive field and find the optimal geometrical features (size, orientation, speed of movement, etc.) for each cell; (ii) random dot backgrounds, made of 1000 random dots covering the whole screen and moving tangentially in different directions; and (iii) optic flow fields, made of 1000 random dots moving radially, with different local speeds, in order to simulate expansion or contraction of the whole field, with centered or shifted foci of expansion.

These tasks were used to assess the relationships between cell activity and retinal signals concerning target localization, preparatory activity for hand movement, hand and eye position and movement direction.

Different activity types were studied: (i) hand-movement related, if cells showed significant changes of firing frequency (see Data Analysis) during Reaction and Movement Time (RMT) of the RF task; (ii) hand-position related, if these changes of activity were observed during Target Holding Time (THT) of the RF task; (iii) activity related to planning hand movement, if cells fired during D_3 of the Instructed-Delay Reach task; (iv) eye-movement related, if modulation occurred during RMT of the Saccade task; (v) eye-position related, if neuronal modulation was found during THT of the Saccade task; the identification of the above-mentioned (i–iv) activity types depended critically on the assessment that neuronal modulation during these epochs did not merely depend on the stimulation of a visual receptive field; and (vi) visual related, when modulation of activity was seen during stationary stimulus presentation and/or during stimulus motion in the visual field. The term 'combinatorial' refers to cells displaying more than one of the above activity types.

Neural Recording

The activity of single neurons was recorded extracellularly through a seven-channel multielectrode recording system (System-Echkorn, Thomas Recording, Marburg). The electrodes were glass-coated tungsten–platinum fibers (1–2 MΩ impedance at 1 kHz), which in some occasions were labeled with the fluorescent carbocyanines DiI or DiI-C5 (Molecular Probes, Eugene, OR, USA), to facilitate reconstruction of the microelectrode penetrations on the histological material.

Data Analysis

Analysis of Neuronal Activity

The average firing rate during different epochs of each task was calculated for each trial. The data were analyzed by using the repeated measures models provided by the 5V program of the BMDP statistical package (Statistical Software, Berkeley, CA, USA). Two different models (Wald's chi-square test) were used for this analysis. In the first, each epoch of interest was compared with the control time. This was a one-factor (task epoch) model with two levels (control time versus task epoch). In the second, both task condition and direction were considered. This model tested, for each epoch, significant differences (i) between two task conditions and (ii) across eight different movement directions (or across eight different target locations, for those epochs characterized by static holding of eye and/or hand). Therefore, these models were used to assess (i) significant modulation of cell activity during different epochs (or combinations of them, i.e. reaction and movement time, RT + MT = RMT) of the same task, relative to the control time (first model); (ii) significant changes of cell activity with movement direction and/or static position of the eye and/or of the hand, or with direction of motion of the visual stimulus (second model); and (iii) differences of cell activity across similar epochs of different task conditions (second model). The interaction term (task × direction) of the second model was used to assess differences in the directional properties of cells across task conditions. The significance level for all statistical tests was set at $P < 0.05$.

Maps of cell activity from the Visual Fixation task were created off-line

to determine location and extent of the visual receptive field of individual cell.

Directional Relationships

A cosine tuning function with adjustable width was used to describe the relationships between cell activity and direction of movement (Battaglia-Mayer *et al.*, 2000).

Several preferred directions were obtained for each neuron, depending on the number of epochs in which the cell was directionally tuned ($R^2 \geq 0.7$) during the Reach, Reach-Fixation, Instructed-Delay Reach (l–d) and Saccade tasks. The mean direction of the sample of preferred directions was given by the orientation of the mean vector (Batschelet, 1981). The length of this vector, the mean resultant length, is a measure of the degree of clustering of the preferred directions. It lies in the range (0, 1), where increasing values correspond to an increasing degree of clustering. The Rayleigh test of randomness (P<0.05) was performed to assess whether the distribution of the preferred directions of each neuron was unimodal. For cells with a unimodal distribution, the angular deviations (Batschelet, 1981) were calculated as

$$s \text{ (degrees)} = (180°/\pi) \, [2(1 - r)]^{1/2}$$

where r is the mean resultant length.

At the population level, the Rayleigh test was performed on the cells' mean directions to assess the uniformity of their distribution.

Analysis of the Tangential Distribution of the Activity Types across PEc and V6A

The tangential distribution of different activity types (hand movement, hand position, planning hand movement, eye movement, eye position, visual) was obtained by aligning in the antero-posterior (AP) dimension of the cortex the cells displaying significant modulation to one or more of these signals. Cell location was determined by taking into account both the chamber coordinates and the location of the 'fluorescent' microelectrode penetrations used as reference, and identified on the histological sections. The medio-lateral (ML) span of our microelectrode penetrations was ~6.5 mm, while the antero-posterior extent was ~14 mm. Cells recorded at different depth and ML locations were assigned to, and therefore 'collapsed' onto, a single coordinate on the AP axis of the cortex, on the basis of their AP coordinates. The 14 mm AP line was then divided into 1 mm wide bins, with the zero corresponding to the middle of the crown of the rostral bank of the POS (parieto-occipital sulcus; Fig. 10). Thus, negative values on the line refer to locations within the bank (area V6A), while positive values indicate locations on the curvature of the sulcus and on the exposed part of the superior parietal lobule (SPL; area PEc). The distribution of parietal association cells projecting to different sectors of premotor cortex [F7, F2 pa, F2 pre-CD (Marconi *et al.*, 2001)] was obtained in a similar way. All retrogradely labeled cells identified in layers II–VI, at different ML level of areas PEc and V6A, were 'projected' onto a 14 mm AP line, and their locations were plotted as frequency distribution (1 mm wide bin). In such a way, physiological and anatomical data were represented on a common axis (the AP tangential domain of the SPL). This made possible their quantitative characterization and comparison, which was performed through the spectral and coherency analysis, in a way similar to that illustrated in the companion study. It is worth noticing that the bin size used (1 mm), while adequate for the physiological data, did not allow sufficient spatial resolution to investigate fluctuations in the number of retrogradely labeled cells with periodicity ~500 μm. These were characterized in the companion paper. Such a high resolution was not necessary for the purposes of the present analysis.

Results

Behavioral Data

During the neurophysiological recording session, the monkeys performed the different tasks at ~90% correct trials. The analysis of the duration of RT and MT of both hand and eye revealed significant differences (Student's t-test, $P < 0.001$) across task conditions. In all instances and behavioral tasks, the RT and MT of the eye were significantly shorter than those of the hand. In the R task, average eye and hand RTs were ~150 and 265 ms, respectively, and eye MT lasted 36 ms. Therefore, hand reaching started ~79 ms after the end of the saccade. Eye RT was shorter when saccades were made in isolation (Saccade task), as compared to when they were made with concomitant occurrence (Reach task) or suppression (Instructed-Delay Reach tasks) of hand movement. The hand RT was longer during reaching to foveated targets (Reach task), when the hand moved after the eye, than during reaching to extrafoveal targets, when fixation was kept constant at the center of the workspace (Reach-Fixation task). On the contrary, the MT was shorter in Reach than in the Reach-Fixation task, resulting in a constant value of the RMT (RT + MT), equal to 399 ms for both tasks.

Physiological Properties of Neurons in Areas PEc and V6A

Cells were assigned to PEc or V6A not only on the basis of the architectonic criteria, but also of the anatomical results obtained (Marconi *et al.*, 2001). The border between PEc and V6A was drawn where the number of cells projecting to F2 [caudal part of dorsal premotor area; PMdc, area 6aα (part)] decreased and that of those projecting to F7 [rostral part of dorsal premotor area; PMdr, area 6aβ (part)] increased. We made 182 microelectrode penetrations in area PEc (Fig. 1*B*) of three hemispheres in two monkeys, and 71 in V6A (Battaglia-Mayer *et al.*, 2000).

Neural Activity Types in Area PEc

Ninety-five cells were studied in the R task, 91 in the RF task, 188 in the S task, 113 in the IDR-l (Instructed-Delay Reach task in normal light conditions), 53 in the IDR-d (Instructed-Delay Reach task in total darkness) and 240 in the VF task.

Figure 2 illustrates the different activity types identified in area PEc. Hand-related signals were a major determinant of cell activity, since most cells (67/91, 78%) were influenced by the direction of hand movement (Fig. 2*A*), and by the active position of the hand in space (54/91, 57%; Fig. 2*B*), as seen during RMT and THT, respectively, of the Reach-Fixation task. The neural activities shown in Figure 2*A*,*B* were derived from cells that were not modulated in the Visual Fixation task, therefore they were independent from visual stimulation of a visual receptive field during hand movement and static positioning on the target. A large proportion of cells (74/113, 65%) were related to the planning of hand movement (Fig. 2*C*), as shown by their activity during the instructed-delay time (D_3) of the Instructed-Delay Reach task. The activity shown in Figure 2*C* comes from a cell not modulated during THT of the Saccade task, therefore it is not dependent on eye position signals. The cells showing light–dark difference in Instructed-Delay Reach task were 32/53 (60%) during preparation for hand movement (D_3), 20/53 (38%) during RMT, and 23/53 (43%) during THT. Their activity was probably related to the visual monitoring of hand position and movement direction in the visual field.

Cell activity, recorded in the Saccade task (RMT), was related to the direction of saccadic eye movements in 33/188 (17.5%) of the cells studied (Fig. 2*D*) and, in a larger proportion of them (41%), to the position of the eye in the orbit (Fig. 2*E*). In most of these cases, cell firing started after the eye movement, and reached the maximal discharge rate within the first 600 ms past the saccade. Thereafter, the discharge ceased or the cell kept firing tonically at a lower rate. Saccade-related neurons showed a clear directional tuning during eye movement (Fig. 2*D*) and

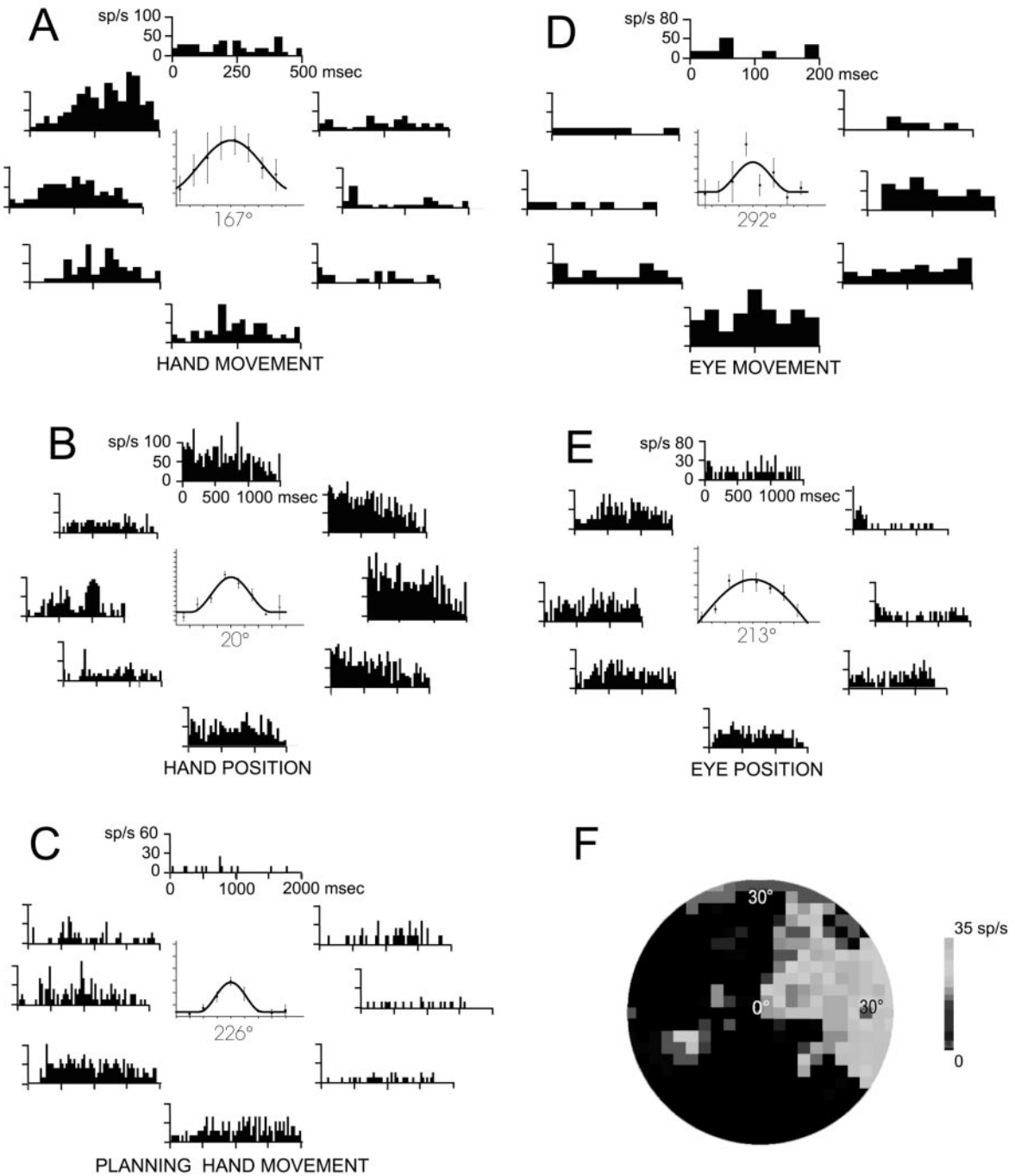

Figure 2. Retinal-, eye- and hand-related signals in area PEc. Peri-event time histograms (*A–E*) and bit-map (*F*) of neuronal activity types obtained by selecting cell activity during given task epochs. (*A*) The activity of one neuron during reaction (RT) and movement (MT) time in the Reach-Fixation task is aligned to the presentation of the peripheral target. In this and following graphs (*B–E*) the directional tuning curves are shown at the center of the family of histograms. (*B*) The activity of another neuron during hand static holding on the peripheral targets in the Reach-Fixation task is aligned to the beginning of target holding time (THT). (C) Neuronal activity of another PEc neuron during preparation for hand movement in the Instructed-Delay Reach task is aligned to the presentation of the instruction signal. (*D*) Neural activity during eye RT and MT in the Saccade task is aligned to the presentation of the visual target. (*E*) Cell activity during eye static holding on different peripheral targets is aligned to the beginning of target holding time. Bin size for histograms is 25ms in (*A*), 30ms in (*B*), (*C*), (*E*), and 10ms in (*D*). (*F*) Activity map of the visual field showing the location and extent of the visual receptive field of one cell, as obtained during inward motion of the visual stimulus in the Visual fixation task. The receptive field extends mostly over the contralateral upper quadrant of the visual field and, to a small extent, over the contralateral lower quadrant as well.

holding of eye position (Fig. 2*E*), with various depths of the tuning curves in different cells. About two-thirds of them did not show any visual response to the stimuli used in our tests.

Cells displaying visual properties were a large fraction of the population studied. Visual receptive fields (Figs 2*F*, 4) were generally large, extrafoveal, and extended over the periphery of the visual field. Cell activity was related to the direction of motion of conventional visual stimuli, with opponent vector

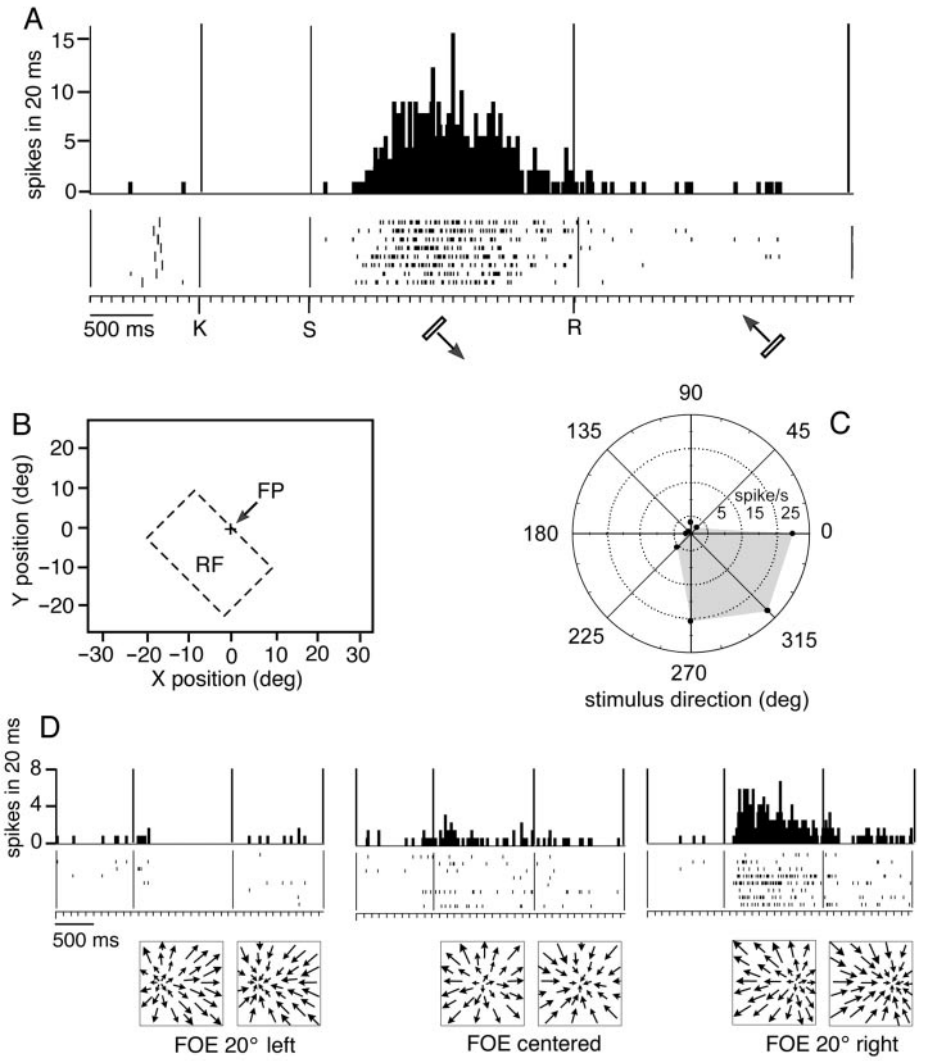

Figure 3. Visual sensitivity of neurons in area PEc. (*A*) Example of neuronal responses to conventional visual motion. Upper and lower plots represent the cell discharge, in form of peri-event time histograms and raster dot, respectively, of eight replications of conventional visual stimulation by a luminous bar (3°×0.4°) moving across the receptive field, while the animal fixated the center of the screen. The time scale reports the salient events of each trial: K, key down after the target presentation (long ticks in the raster dot); this is the synchronization event for the trials. During the time period K–S, the animal fixates without any visual stimulation. The bar appears and starts moving at time S; then, after a complete sweep across the receptive field, it inverts its direction (R) and moves in the opposite way. The directions of this example are those indicated by the arrows below the raster dot. (*B*) Position and extension of the receptive field, relative to the fixation point (FP). (*C*) Polar plot of mean discharge rates of responses to bars moving across the receptive field, along eight directions. This cell exhibits classical visual motion sensitivity, with direction selectivity. (*D*) Example of responses to radial optic flow. Each panel shows the cell discharge in response to a random dot background, expanding or contracting, with focus of expansion (FOE) at different positions with respect to the fixation point. It is clear how the cell is excited by the expansion centered to the right of FP and is suppressed by the same event centered to the left.

organization (Motter and Mountcastle, 1981) of the response properties in many cells.

Visual Properties of Neurons in Area PEc

Two hundred and forty cells of area PEc were tested during the Visual Fixation task. Out of these, 107 (44.6%) were responsive to visual stimulation. Seventy-eight cells were studied in a rigorous quantitative way. The majority of them (73/78; 93%) discharged when conventional solid bars were moved within a classical receptive field. Figure 3*A–C* shows an example of such a visual sensitivity. Direction selectivity was present in 86% of the neurons tested (67/78), with opponent responses to opposite directions (directionality index, 1 – null direction/preferred direction ≥ 0.5). Size, orientation or luminous contrast of the stimuli did not modulate the visual responses. In these cells, the receptive fields were usually quite large, often including a quadrant or a hemifield of the screen. Recordings failed to show any evident retinotopic order, since the centers of the receptive fields of nearby cells in the same electrode penetration jumped from peripheral to central retinal locations without any orderly sequence. Figure 4 shows two representative electrode tracks in PEc, where visual motion related cells and their receptive fields are described. Along these tangentially oriented penetrations, the preferred directions of stimulus movement did not appear to shift in a systematic way between neurons recorded within the same electrode penetration. The sensitivity to optic flow stimulation was studied in 78 visual cells. A substantial number of them (35/78; 44.8%) were responsive to radially expanding or contracting optic flow, with preferred shift of the focus of expansion (FOE). Figure 3*D* reports a clear example of this property. In this instance, the preferred FOE was to the right of the fixation point, while FOE to the left gave suppression of cell

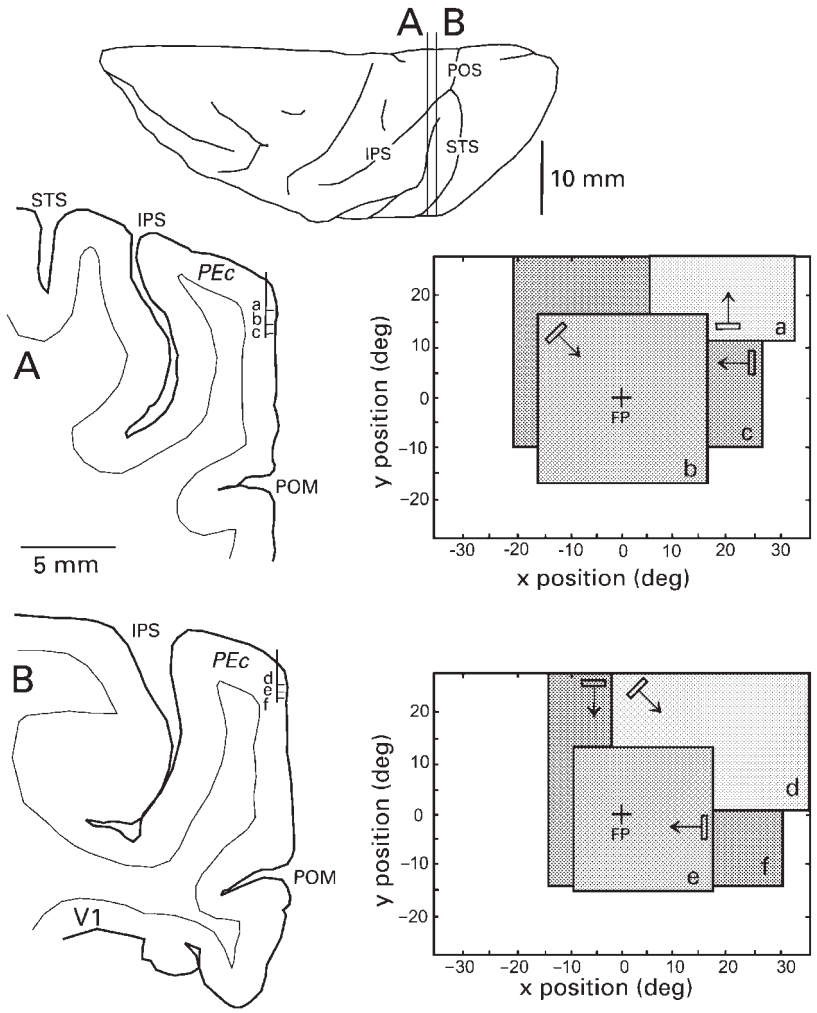

Figure 4. Visual receptive fields of neurons in area PEc. Top – dorsal view of the monkey's brain. A and B in the brain figurine indicate the approximate level of the corresponding histological sections shown below with the reconstruction of the electrode tracks in area PEc. Small tacks (a–f) are recording sites where motion-sensitive cells were found. On the right, a–f indicate the corresponding visual receptive fields. FP, fixation point. Arrowed bars show the preferred direction of each cell. IPS, intraparietal sulcus; POM, medial parieto-occipital sulcus; POS, parieto-occipital sulcus; STS, superior temporal sulcus; V1, striate cortex.

discharge. Although luminous bars usually excited these cells, the specific expanding or contracting stimulus, whose spatial features could not be predicted by the responses to local motion, elicited their optimal discharge. Responses to translation of the whole random dot background were solely weak or absent in PEc.

Neural Activity Types in Area V6A

The neural activity types (Fig. 5) observed in area V6A were basically similar to those of PEc. Retinal, eye, hand position and movement direction signals were common in this area, although for some of them, the relative weight was different in the two areas. The main difference was observed in the higher proportions of eye-related neurons in V6A, where saccadic eye movements and eye position modulated, respectively, 25% and 68% of the cells studied. A full description of the dynamic properties of neurons in area V6A is offered in another study (Battaglia-Mayer *et al.*, 2000).

Directional Tuning Properties of Neurons in PEc and V6A: Global Tuning Fields

The multi-task approach adopted in this study revealed that different eye- and hand-related signals often coexisted in the same cell, although with different combinations in different cells. Two examples are shown in Figure 6. The cell studied in area PEc was directionally tuned during different epochs of different tasks. In the Reach task, this cell was directionally tuned during hand movement time (MT), and during combined eye–hand holding on the targets (THT). In the Reach-Fixation task, cell activity was tuned during hand RT and MT, and during static hand holding on the targets (THT). In the Saccade task, the directional tuning was not significant. In the Instructed-Delay Reach task, this cell's activity was related to the direction of eye movement (D_2), to that of the intended (D_3) and real (RT, MT) hand movement, and to combined eye–hand position on the targets (THT), with no major differences between light and dark conditions.

When the preferred directions obtained from all these different epochs were represented on a unit circle, a remarkable feature of the directional properties of this cell emerged. The orientations of these preferred directions clustered within a limited sector of space, the field of global tuning (Battaglia-Mayer *et al.*, 2000), which was defined on the basis of the unimodal distribution (Rayleigh's test, $P < 0.05$) of preferred directions.

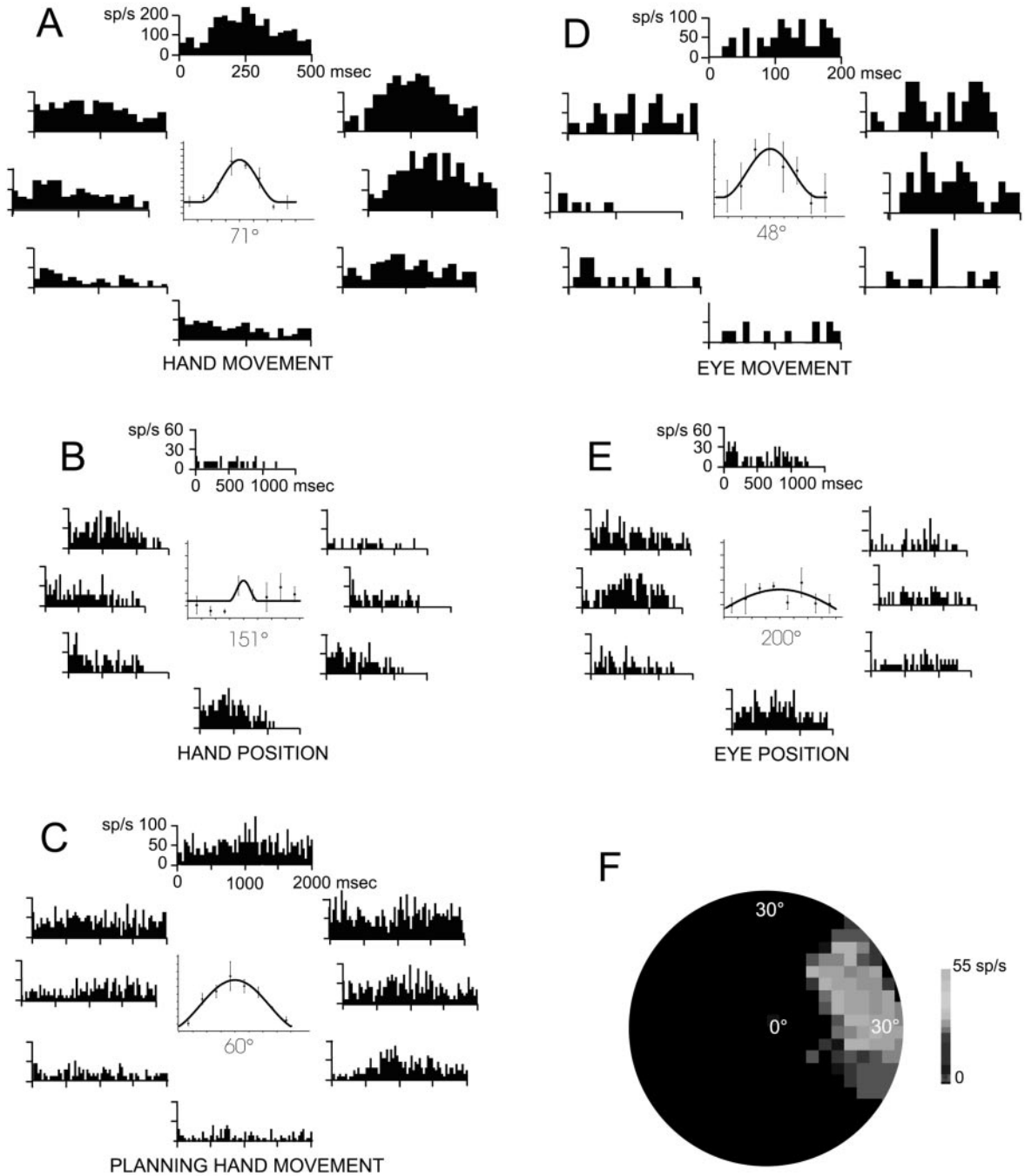

Figure 5. Retinal-, eye- and hand-related signals in area V6A. The activities shown in (*A*) and (*B*) were derived from cells that were not modulated in the Visual Fixation task, therefore they were independent from visual stimulation of a visual receptive field during hand movement and static positioning. The activity shown in (*C*) comes from a cell not modulated during THT of the Saccade task, therefore it is not dependent on eye position signals. Conventions and symbols are as in Figure 2.

For the neuron of area PEc, the mean resultant vector was oriented at 336°. The mean resultant length was 0.95, indicating a very high degree of clustering.

The relationships of individual neurons to different retinal-, eye- and hand-related signals in V6A were very similar to those observed in PEc, and so were the global tuning fields (Fig. 6).

Global Tuning Fields of Parieto-occipital Neurons: a Population Analysis

A large proportion (58%) of cells in area PEc had significant global tuning fields, as determined on the basis of the unimodal distribution of cell's preferred directions.

Representative examples of global tuning fields of parieto-occipital neurons in area PEc are shown in Figure 7. A population analysis is offered in Figure 8. For this analysis, the mean resultant vector and its length for each global tuning field were calculated. The mean resultant length was different for different cells, as shown in Figure 7. The frequency distribution of the angular deviations (Fig. 8*A*) illustrates the limited spread of the preferred directions around the mean vector. All the cells of

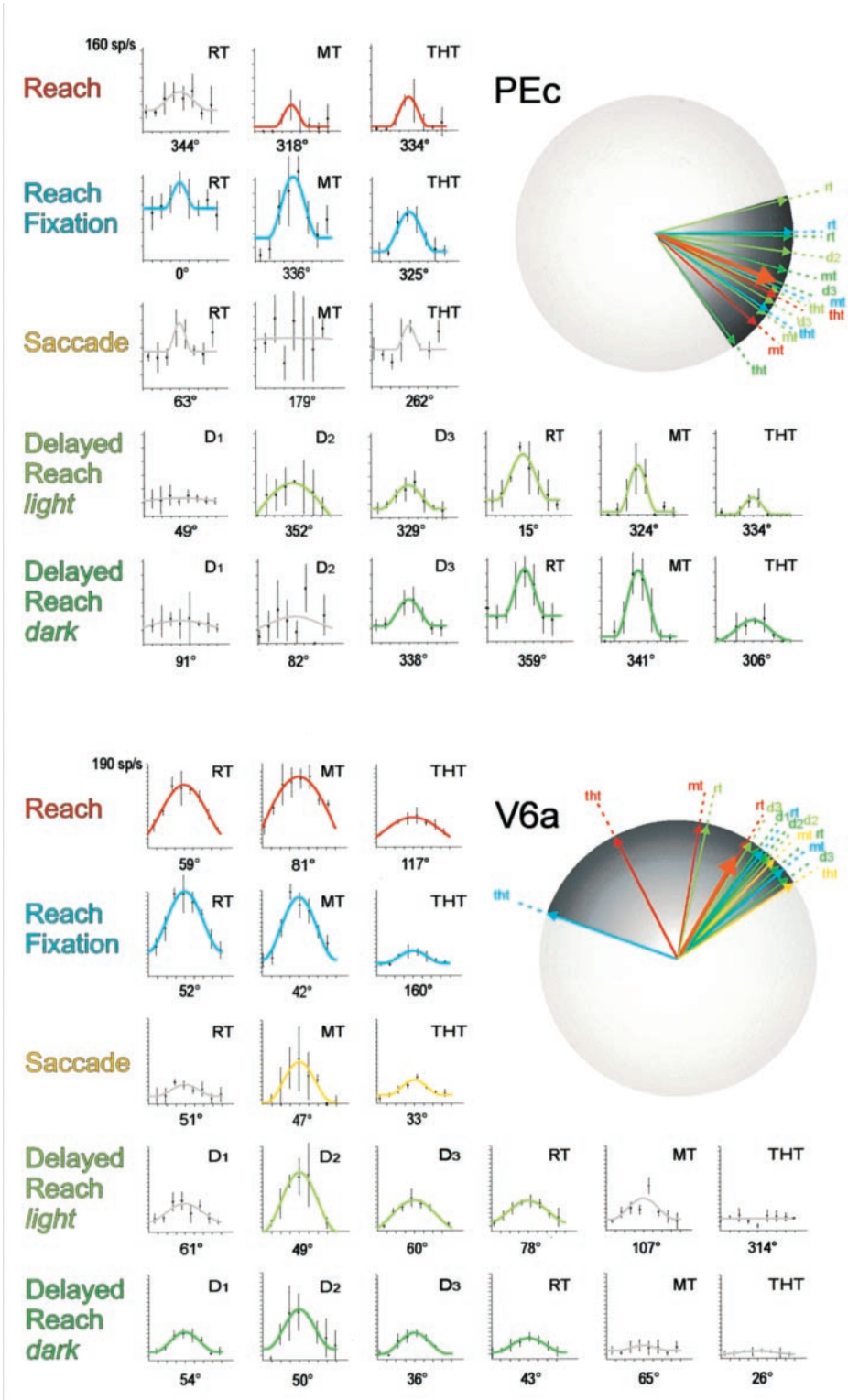

Figure 6. Directional tuning curves (centered on their preferred directions) across different epochs of different tasks and global tuning fields (unit circles on the right) of two neurons, one from PEc, the other from V6A. In the Reach, Reach-Fixation and Saccade tasks, RT, MT and THT indicate reaction-, movement- and target-holding time, respectively. In the first two tasks, the RT refers to the hand behavior, in the third, to the eye behavior. In the Delayed-Reach task, D_1 and D_2 refer to the eye reaction time and movement time, D_3 indicates the instructed-delay time, and RT, MT and THT are as in the previous reaching tasks. The vectors of unit length in the global tuning field are represented in different colors corresponding to different tasks and point to the preferred directions of the epochs indicated by the labels. The thick orange arrow indicates the mean resultant vector, the length of which (the mean resultant length) indicates the spread of the global tuning field.

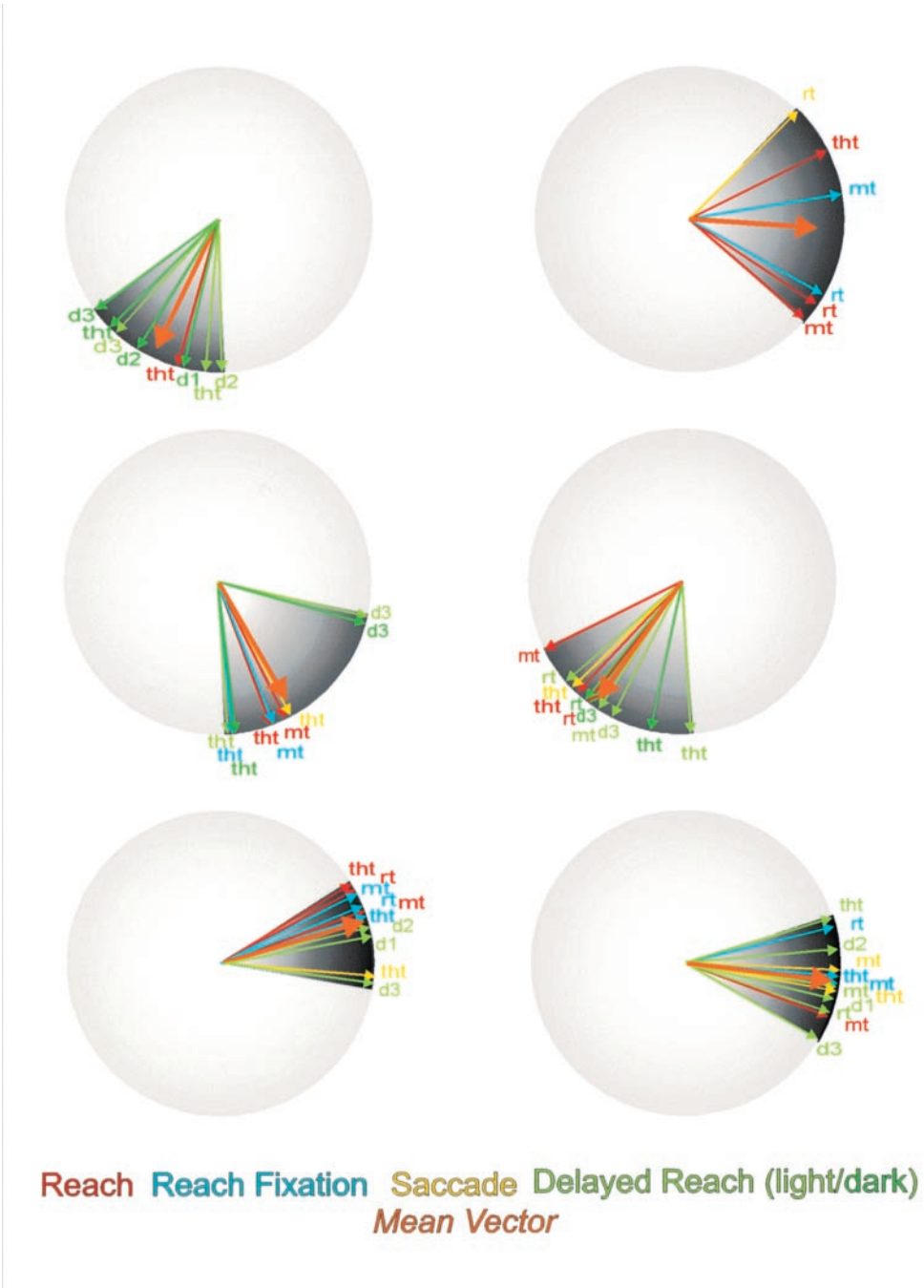

Figure 7. Global tuning fields of six different cells in area PEc. Conventions and symbols as in Figure 6.

Figure 8*A* had a unimodal distribution of their preferred directions. At the population level (Fig. 8*B*), the angles of the mean resultant vectors, the mean directions, were isotropically distributed in space (Rayleigh's test), suggesting that the eye and hand directional continuum is represented in a uniform way in the activity of the population of parietal neurons studied.

Context Dependency of Hand and Eye Movement Related Activities

A very common observation in both PEc and V6A was the context dependency of cell activity. An example is offered (Fig. 6) by the difference in firing frequency (PEc) or directional tuning (V6A) during hand movement (MT) of the Reach and Instructed-Delay Reach task, in normal light conditions. In both cases, during hand MT, the eye was on the target, and the hand movement had the same origin and endpoint. However, in the Reach task the animal moved the hand as soon as he could within a 'reaction-time' paradigm, while in the Instructed-Delay Reach task target location was pre-cued by an instruction signal, and, therefore, reaches could be planned well in advance. Furthermore, in the first task, the eye and the hand moved in rapid sequence, while in the second, hand movement occurred after an intervening long temporal delay.

Figure 9*A* shows another case, from V6A, where histograms of cell activity, together with the relative directional tuning curves, were superimposed for the two tasks. Not only the amount of

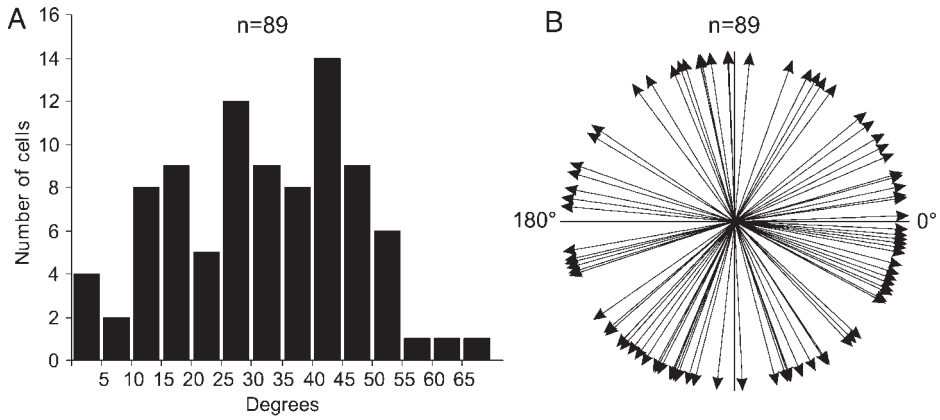

Figure 8. Global tuning properties of parietal neurons. Frequency distribution of the angular deviations (*A*) and mean directions (*B*) of parietal (PEc and V6A) cells ($n=89$) with significant global tuning field (Rayleigh test, $P< 0.05$).

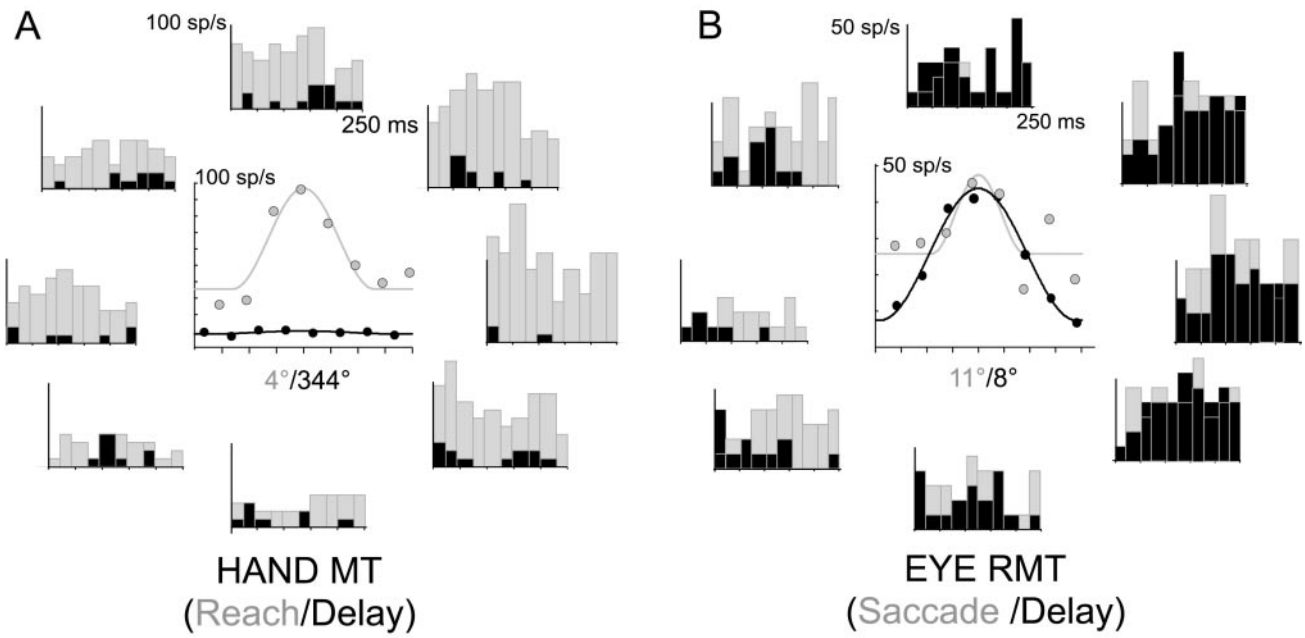

Figure 9. Context dependency of cell activity in areas PEc and V6A. (*A*) Histograms (bin size 25ms) of cell activity during MT of the Reach (gray) and Instructed-Delay Reach (black) tasks are aligned to onset of hand movement. In the center, the relative directional tuning curves are shown. During MT of the Reach task, $R^2 = 0.9$; during MT of the Instructed-Delay Reach, $R^2 = 0.3$. (*B*) Histograms (bin size 25ms) of cell activity during saccadic eye movement in the Saccade (gray, RMT) and Instructed-Delay Reach (black; $D_1 + D_2$) tasks are aligned to target presentation. In the center, the relative directional tuning curves are shown. During RMT of the Saccade task, $R^2 = 0.64$, during $D_1 + D_2$, $R^2 = 0.98$.

activity (Wald's test, $P < 0.05$), but also the directional relationships (Wald's test, task × direction interaction term, $P < 0.05$) and the directional tuning of this cell changed during hand MT across task conditions.

In area PEc, out of 79 cells studied in both Reach and Instructed-Delay Reach (light) tasks, and modulated in at least one task during MT, 15 (19%) were active only during delayed reaches, 21 (27%) were modulated only during standard reaches, and 43 (54%) fired significantly in both tasks. Out of these, 37 (86%) showed significant changes of activity during MT when compared across tasks. Similar results were obtained in V6A, where the cells modulated during hand MT in both tasks were 42, out of which 35 (83%) showed significant changes of activity across tasks.

Not only hand-movement, but also eye-movement related activity was task dependent, as can be seen by comparing cell firing during saccadic eye movements in two conditions, in absence of future hand movement (Saccade task), and when, after a delay time (Instructed-Delay Reach task), the animal made hand movement toward an already foveated target, and therefore, to the fixation point. The PEc cell of Figure 6 offers an example, since it was silent during eye movement (MT) in the Saccade task, while it displayed a significant directional tuning during the same eye movement (D_2) in the IDR-l task. The cell of Fig. 9*B* (from PEc) shows that the amount of activity (Wald's test, $P < 0.05$) changed and the directional tuning curve scaled during eye movement across task conditions.

In the parieto-occipital cortex, out of 99 cells studied during the Instructed-Delay Reach task and in the Saccade task, and modulated in at least one task during eye RMT, 45 (46%) were modulated only in the Instructed-Delay Reach task, 18 (18%) only in the Saccade task, 36 (36%) in both tasks. Out of these 24

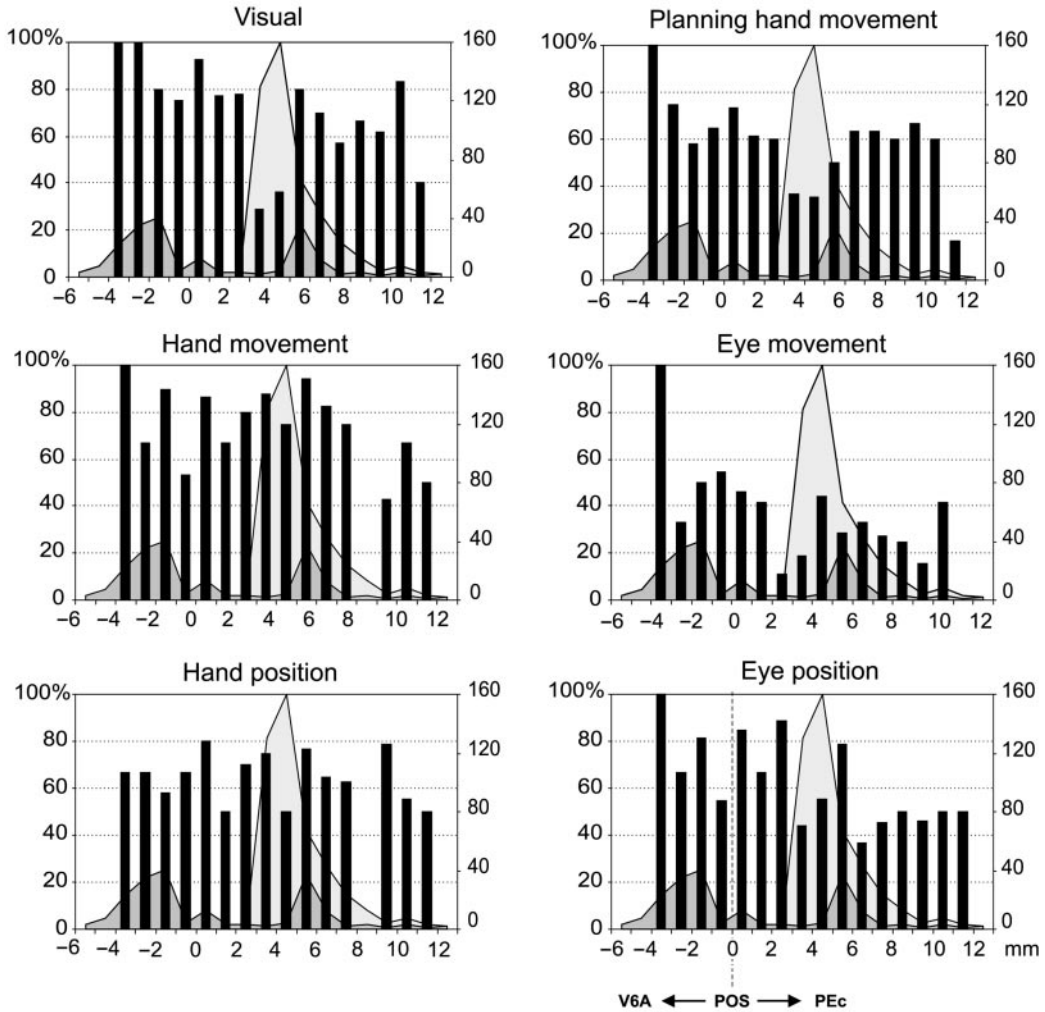

Figure 10. Tangential (antero-posterior) distribution of both activity types (black columns) and parieto-frontal association cells (gray areas) projecting to F7 and F2, across areas PEc and V6A. The abscissa represent the AP domain with 0 corresponding to the middle of the crown of the POS. Negative values on the abscissa refer to locations within the bank (area V6A), while positive values indicate locations on the curvature of the sulcus and on the exposed part of the SPL (area PEc). The percentage of cells, out of those recorded at a certain AP level, with significant modulation of neural activity during different epochs of the behavioral tasks, and therefore expression of the processing of different signals, are represented as frequency distributions (left ordinate). Similarly, the number of cells retrogradely labeled from injections in F7 (dark gray) and F2 (light gray) was counted (right ordinate) and contrasted to that of different activity types. Bin size is 1mm for all distributions.

(67%) showed significant differences in cell activity across task conditions.

Distribution of Neural Activity Types across PEc and V6A. A Comparison with the Distribution of Parietal Cells Projecting to the Frontal Cortex

The region of significant (Wald's test, $P < 0.05$) task-related activity explored in this study extended for ~14 mm in the antero-posterior extent of the SPL, encompassing both areas PEc and V6A. The distribution of the physiological activity types identified was contrasted to the anatomical distribution of the retrogradely labeled cells projecting, from the region of physiological recording, to dorso-rostral (F7), or dorso-caudal {F2 pre-CD [area F2 lateral to the pre-central dimple; area 6aα (part)]} premotor cortex (Fig. 10).

The overall anatomical distribution of parietal cells projecting to premotor cortex was not uniform, since their number waxed and waned in a periodic fashion. A similar periodic arrangement was observed in the distribution of physiological activity types.

The number of visual-related cells was high where the labeled cells projecting to F7 were more numerous, and low where these association cells were scarce. This was observed in both V6A and PEc. Furthermore, few visual-related cells were observed in the region where the projection to F2 was largely dominant.

The distribution of cells with neural activity related to the planning hand movement in the IDR task closely resembled that of visual activity. Hand-movement related cells were abundant in the parietal region containing the maximal number of cells projecting to F2 pre-CD. Beyond this, little orderly relationships was seen between hand movement cells and projections to frontal cortex.

Although the overall number of eye-movement related cells was rather small across the region of recording, their distribution showed a clear periodicity, with two main peaks aligned to those of parietal cells projecting to F7.

Finally, hand- and eye-position related activities were distributed in a more continuous fashion across V6A and PEc, and encompassed the parietal regions projecting to F7 and F2 pre-CD in a rather even way.

It is important to stress that the distribution of each of the

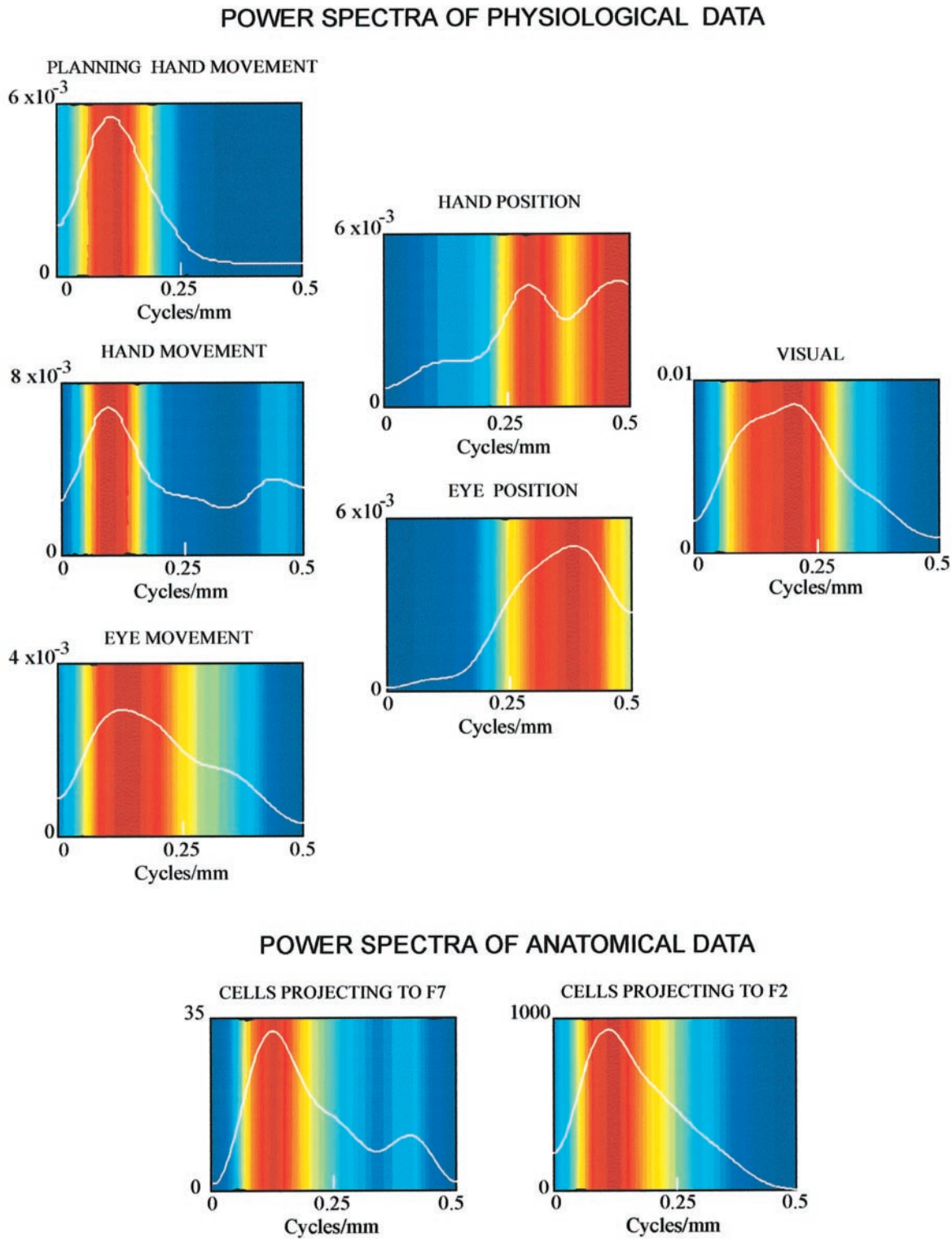

Figure 11. The spectral analysis of physiological data was performed on the distributions of cells with different activity types, across areas PEc and V6A. The power spectrum is represented in the form of an autoperiodogram (white line) that is superimposed to a color-coded image of the same spectrum, where the dark red corresponds to peak. The spectral analysis of anatomical data was performed on the distributions of the parietal cell retrogradely labeled by the injections in F7 and F2, and that were found within the region of physiological recording.

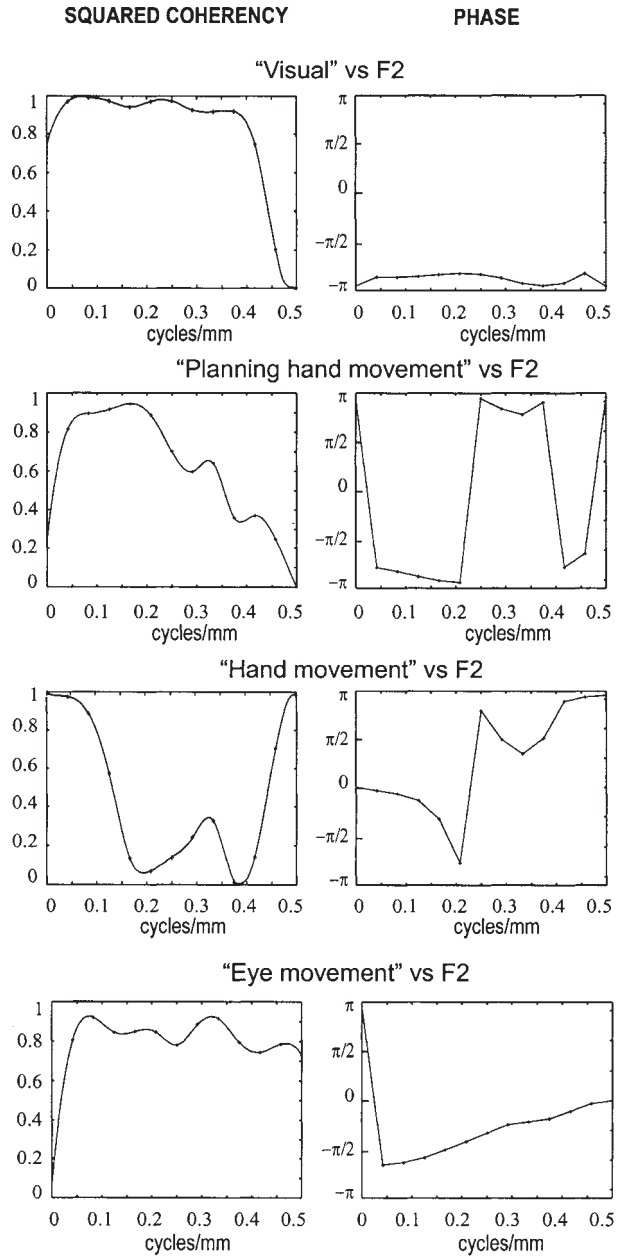

Figure 12. Coherency analysis and phase relationships between the distributions of parietal cells projecting to F2 and those of different activity types, as a function of Fourier frequencies (cycles/mm). The squared coherency of the cross spectrum varies from 0 to 1, and the phase between the individual spectra varies between $-\pi$ and π. The activity types analyzed (ANOVA) were visual activity (from the Visual Fixation task), activity related to planning of hand movement (from the delay time D_3 of the Instructed-Delay Reach task), hand movement activity (from RT and MT of the Reach-Fixation task) and eye movement activity (from RT and MT of the Saccade task).

physiological activity types illustrated above was broader than that of the cells retrogradely labeled, so that the two distributions overlapped only over a limited tangential extent of the cortex. This implies that the information encoded by these neural profiles is probably available also to other cortical efferent systems.

The periodic distributions of both labeled cells and functional properties were characterized and compared through a spectral analysis (Figs 11–13), which revealed an orderly organization of the power spectra of the different activity types. The spectra (Fig. 11) referring to the distributions of the cells with significant task-related activity during planning of hand movement, hand movement and saccadic eye movements were dominated by a main common elevation in the domain of the low spatial frequencies, with a peak at ~0.1 cycles/mm. This indicates that both hand- and eye-movement related cells share a periodic distribution with peak-to-peak distance of ~10 mm [1/(0.1 cycles/mm) = 10 mm]. This implies that these cells are arranged in bands 5 mm wide.

Contrary to that illustrated above for the movement-related activities, the distributions of cells with position-related activity, either eye or hand, were characterized by power spectra with predominant elevations in the domain of the high spatial frequencies. In particular, the spectrum of hand-position cells had two peaks, at 0.29 and 0.45 cycles/mm, which correspond to clusters of cell density 1.7 and 1.1 mm wide, respectively.

The power spectrum of the distribution of cells with significant visual activity was dominated by a strong elevation in the domain of the low spatial frequencies peaking at 0.20 cycles/mm, which correspond to bands of 2.5 mm.

Concerning the anatomical distributions of parietal cells projecting to F7 and F2 from the region of physiological recording, the main common feature of their power spectra was a prominent elevation in the domain of the low Fourier frequencies, with a common peak at ~0.1 cycles/mm. This corresponds to a periodicity in cell density, in the antero-posterior extent of the cortex, with a peak-to-peak distance of 10 mm, and therefore to bands of association cells of ~5 mm.

Anatomical and physiological distributions were compared through the coherency analysis (Figs 12 and 13). The coherency of the cross-spectrum provided a measure of the similarity of the two distributions in the frequency domain, while the phase provided a measure of their spatial relationships, but only in the domain where the coherency of the cross-spectrum was high [see Materials and Methods section in the companion paper (Marconi *et al.*, 2001)].

The spectrum of the distribution of association cells projecting to dorso-caudal premotor cortex (F2, PMdc) was contrasted to the spectrum of the distribution of each of the physiological activity types (Fig. 12). When the distribution of visual activity was considered, the coherency was high at almost all spatial frequencies (0–0.4 cycles/mm). However, at these same frequencies, the two distributions were completely out of phase. This indicates that the periodic components (bands and clusters) of the distribution compared were very similar, but segregated in space. When the spectrum of the distribution of signals concerning planning of hand movement was taken into account, the coherency of the cross spectrum was high only at the low spatial frequencies (0–0.2 cycles/mm), and the two distributions were out of phase. The cross spectrum with hand movement signals had a very high coherency at the very low spatial frequencies (0–0.5 cycles/mm). In this frequency domain, the bands of association cells were almost perfectly in phase with, and therefore aligned to, those of hand-movement related cells. Finally, the coherency of the cross spectrum with eye movement signals was high at most spatial frequencies (0.075–0.5), and the two distributions were out of phase. Therefore, only the bands of cells with significant hand-movement activity overlapped in space with that of parietal cells projecting to dorso-caudal premotor cortex (F2).

The comparison of the spectra of the different activity types with the spectrum of parietal cells projecting to dorso-rostral premotor (F7) cortex (Fig. 13) showed that this last distribution

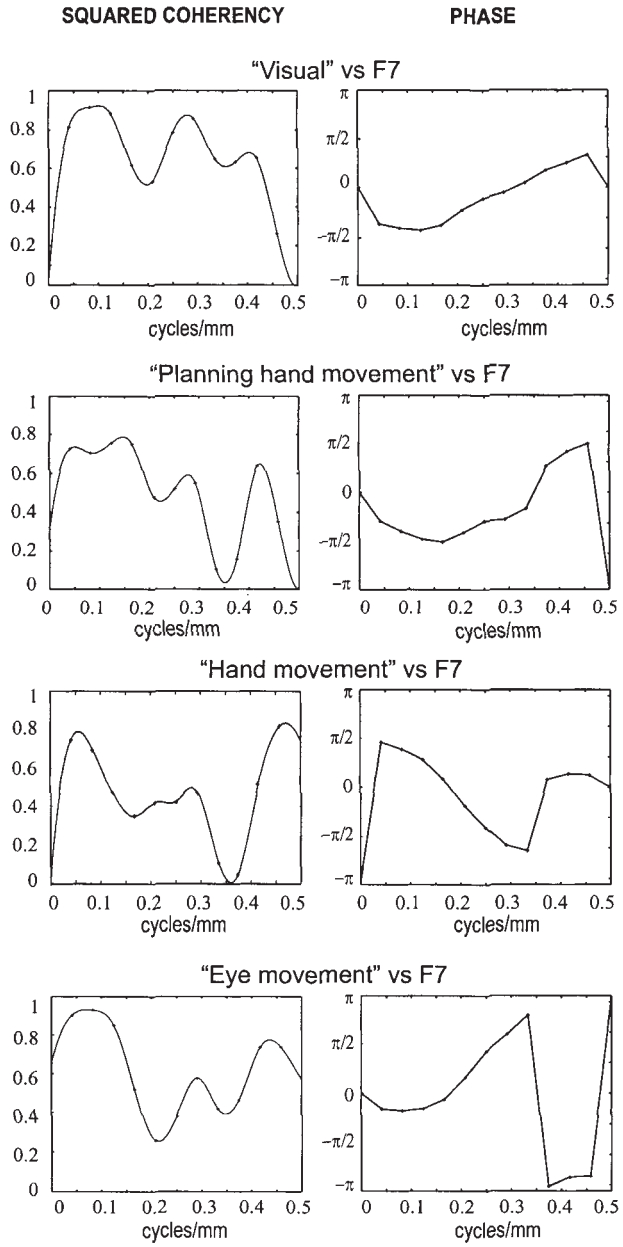

Figure 13. Coherency analysis and phase relationships between the distributions of parietal cells projecting to F7 and those of different activity types, as a function of Fourier frequencies (cycles/mm). Conventions and symbols as in Figure 12.

was spatially aligned with those of cells with saccadic activity, while slightly (90°) out of phase with the distribution of visual, and hand movement information concerning both planning and execution.

Discussion

The Parieto-occipital Cortex and Visuomotor Behavior

In this study, behavioral neurophysiology was combined with neuroanatomy to achieve a functional characterization of some of the parietal regions reciprocally linked with dorsolateral premotor cortex. This was a necessary step to attempt an interpretation of the functions of parieto-occipital cortex and of the association connections shared with premotor cortex. These functions, in fact, can hardly be understood in terms of topographic representation. This difficulty lies in the absence of orderly arranged, fine-grain representations of the sensory peripheries in the tangential domain of the parietal cortex, and in the highly conditional and task-dependent nature of parietal cell activity.

In both V6A and PEc, retinal-, eye- and hand-related signals are all combined in the activity of most cells. Therefore, these areas are part of a distributed network that process, though to a different degree, signals for various forms of eye–hand coordination.

The visual properties of neurons in this part of the SPL, i.e. the large peripheral receptive field, the sensitivity to direction of stimulus motion, the opponent vector organization of their response to visual motion (Motter and Mountcastle, 1981), are ideally suited for the process of visual perception of moving objects, including the hand, in the visual field. Therefore, these populations of neurons can play an important role in the visual monitoring of the position and movement of the hand in the field of view. The sensitivity to optic flow fields suggests a role in the analysis of self-motion, which could be important when combined eye–hand actions are made while walking, another very common form of daily behavior. These properties assign to areas V6A and PEc a role in ambient vision (Trevarthen, 1968) and in the spatial organization of movement (Caminiti *et al.*, 1996). This is not surprising for V6A, since, as part of area 19, this area has traditionally been considered a visual association cortex. On the contrary, this is a novel finding for PEc, which, in absence of any physiological study and based on cytoarchitectonic criteria, has been regarded as a somatosensory association cortex.

Global Tuning Fields as Combinatorial Domains for Eye–Hand Related signals

There is general consensus that coding visually guided hand reaching requires a combination of different information. Psychophysical data in humans (McIntyre *et al.*, 1997, 1998) suggest that in this process a visual target is first represented in an eye-centered reference frame, with a characteristic distortion of perceived distances along the sight line, and then transformed into an arm-centered representation, with another associated distortion in the arm-linked reference frame.

Psychophysical studies have also shown a powerful coupling between eye and hand behavior during different phases of reaching, and under a variety of experimental circumstances (Neggers and Bekkering, 2000). This also emerges in our study, from the analysis of monkeys' eye and hand reaction and movement time across task conditions.

The properties of parieto-occipital (Battaglia-Mayer *et al.*, 2000) neurons can offer a physiological substrate to this combinatorial mechanism. Our results indicate that in the information processing flow leading from vision to movement, the combination of signals occurs at the very early stages, in the parieto-occipital cortex and mesial parietal cortex (Ferraina *et al.*, 1997a,b). Depending on the task demands (Burnod *et al.*, 1999), different combinations of reach-related variables could be achieved, resulting in different forms of eye–hand coordination.

The global tuning field of parietal neurons is a key feature for such mechanism. There are at least four main properties of the global tuning field that suggest its potential role in the early stages of the visuomotor transformation for reaching. First of all, the combinatorial power. The results of the present experiments indicate that within the global tuning field, parietal neurons can combine eye- and hand-related information. This refers to planning eye and hand movement during reaction-time tasks

and, on the contrary, under conditions in which the target location is available well in advance; to actual eye and hand movement and holding of static positions; to signals concerning the sight and, possibly, the monitoring of hand trajectory in the visual field, and, finally, to information relative to the spatial coincidence between the eye and the hand on the fixation point.

Secondly, the spatial nature of the global tuning field, i.e. the directional properties of all information encoded, in terms of both movement direction and position in space, might facilitate the combination of signals on the basis of their spatial congruence. This suggests that within the global tuning fields eye- and hand-related signals can be dynamically recombined to participate in the composition of commands for visually guided reaching.

Thirdly, the contingent and task-dependent relationships between cell activity and different eye–hand related signals are such that many cells display meaningful relationships to eye movement only when the target for the saccade is also target for hand movement; similarly, many neurons relate to hand movement depending on whether or not reaches are made within a reaction-time or an instructed-delay time paradigm. This implies that context dependency is an important factor in the signal composition of the global tuning field. This conditionality refers not only to the nature of the signals processed across the network, but also to their temporal relationships with the evolving behavioral events of a reaching tasks. During the delayed-reach task (Johnson *et al.*, 1996; Kalaska, 1996), in spite of a largely simultaneous recruitment of neurons in both parietal and frontal cortex, parietal cortex leads motor cortex relative to the presentation of the visual cue signal that instructs the animal about the direction of the future hand movement, while motor cortex leads parietal cortex relative to presentation of the visual go signal for hand reaching. Context dependency is a crucial feature, since it allows a flexible combination of signals and assigns to parietal neurons more than a single 'fixed' role within the parieto-frontal network. The consequence is that no 'permanent' assignment of coding schemes (eye-centered, arm-centered, etc.) can be made to parietal neurons. In this view, the concept of reference frame is largely inadequate to face the complexity and richness of the combinatorial capacity of the parietal network.

Fourthly, the global tuning can be found in 2/3 of parietal neurons, and therefore is a general property of the cortex in the SPL.

The Efferent Messages of the Parieto-frontal Network

Insights into the nature of the efferent messages addressed by the parietal lobe to the frontal lobe can be gained by comparing the distributions of activity types and of parieto-frontal association cells in the tangential domain of the cortex. In our study, this comparison was possible thanks to the combined anatomical and physiological approach.

In general, the tangential distribution of both activity types and parieto-frontal cells was uneven in the antero-posterior tangential domain of areas PEc and V6A. Therefore, it was important to characterize them in a rigorous quantitative way. We have adopted a spectral and coherency analysis, since the first detects the spatial periodicities of the distribution of both association cells and activity types, and the second provides a measure of their similarity. The spatial arrangement of the two distributions was studied through the analysis of their phase relationships.

The main result of this analysis was the orderly arrangement of both anatomical and physiological properties in the antero-posterior domain of the SPL. The spectra of the distributions of the efferent cells projecting to dorso-rostral and dorso-caudal premotor cortex were both dominated by a peak in the domain of the low spatial frequencies. The same result was obtained for the spectra of the distribution of the activity types concerning preparation for hand movement, hand movement, eye movement, as well as for the distribution of visual signals. This indicates that parieto-frontal cells and signals concerning the visual and dynamic aspects of motor behavior were both arranged in the form of bands of similar sizes. On the contrary, most of the power spectrum of the distribution of positional signals (eye and hand position) was found in the domain of the high spatial frequencies, suggesting a more patchy arrangement in the cortex, probably in the form of columns.

The coherency analysis revealed that the bands of hand-movement related signals were similar and in phase mainly with those of the cells projecting to dorso-caudal (F2) premotor cortex. This indicates that the two distributions overlap in space. On the contrary, the bands of visual signals and those referring to information about planning hand movement and eye movement were coherent and overlapped in space with those of parieto-frontal cells projecting to dorso-rostral premotor cortex (F7). As a consequence of their rather continuous and columnar arrangement, eye and hand position signals were not coherent with the distributions of either cells projecting to F7 or to F2, which, as already seen, were in the form of bands. This does not imply segregation in space, but only a different periodic arrangement (band-like versus columnar). In fact, the distributions of these positional signals overlapped those of cells projecting to F2 and to F7 over all the tangential extent of parieto-occipital cortex.

In conclusion, this analysis suggests that the architecture of parieto-occipital network underlying reaching can be viewed as a matrix of eye and hand position signals, containing orderly arranged bands of movement-related activity types which match similar bands of parieto-frontal cells. This matching is selective and depends on the activity profile and on the destination of the efferent pathway considered. This spatial match suggests that the functional signals detected by the multi-task approach of this study have probably access to the parieto-frontal system. Visual signals concerning target location, planning hand movement and eye movement have a privileged access to the efferent system addressed to dorso-rostral premotor cortex, while signals about hand movement are mainly addressed to dorso-caudal premotor cortex. Eye and hand positional signals should be available to the parietal projection to both rostral and caudal dorsal premotor cortex. This layout of the parieto-frontal system predicts a predominance of eye-related and preparatory information in the rostral part of premotor cortex, and a preponderance of hand-related signal in its caudal part. This is exactly what has been found by physiological studies addressed at the analysis of signal processing in dorsal premotor cortex (Johnson *et al.*, 1996; Jouffrais and Boussaoud, 1999, Fujii *et al.*, 2000) [for a discussion see (Caminiti *et al.*, 1996, 1998; Wise *et al.*, 1997)].

These results extend to parieto-occipital cortex the gradient-like (Johnson *et al.*, 1996) arrangement of functional properties already shown for parietal areas PE, PEa [parietal area PEa; area 5 (part)] and MIP [medial intraparietal area; area 5 (part)], and for frontal areas PMdr (F7), PMdc (F2; Fujii *et al.*, 2000) and motor cortex. Association fibers connect reciprocally these parietal and frontal areas.

Optic Ataxia as a Consequence of the Breakdown of the Combination of Ocular and Manual Signals within the Global Tuning Fields of Parietal Neurons

The global tuning fields and the gradient-like architecture are general features of the parieto-occipital cortex. Both can be relevant for an interpretation of optic ataxia (Balint, 1909), a common consequence of lesions of the parieto-occipital cortex.

Optic ataxia is characterized by the inability to reach with precision toward a target localized in space by vision (misreaching), and is often accompanied by an erroneous orientation of the hand before grasping an object (Perenin and Vighetto, 1988). This defective visual control of movement extends also to daily life. These patients are unable to correctly light a cigar at its end, they often do it at its center, and when trying to fill a glass of wine, they pour the wine on the right or left, or in front or behind the glass, rarely in the glass. When walking, they often collide with obstacles or objects located in their way. These parietal patients also suffer from a severe impairment of eye fixation and movements (Balint, 1909; Head and Holmes, 1911–1912) [see (De Renzi, 1982) and (Harvey and Milner, 1995), for a review of this early literature]. Interestingly, these patients were able to move and were aware that a movement had occurred, but they were unable to specify its direction (Head and Holmes, 1911–1912). In other words, they were unaware of the direction of movement.

An overview of the literature on optic ataxia is out of the scope of the present study and the possible relationships between the anatomo-functional organization of the parieto-frontal system and this disorder have been addressed in past reviews (Caminiti *et al.*, 1996; Battaglia-Mayer *et al.*, 1998). What we would like to stress in this context is that, from the analysis of the symptoms of parietal patients, a common feature emerges, i.e. the directional nature of their errors. A second important feature is that these disorders only occur when movement is made to a visual target, in absence of 'primary' visual or motor deficits. Therefore, the impairment is context dependent, since it occurs only when eye and hand information are to be combined.

An advance in the interpretation of optic ataxia is now possible on the basis of observation that parietal neurons can combine spatially congruent eye- and hand-related information within the global tuning field; for any given neuron, the nature of the eye and hand signals processed within the tuning field is not fixed, but context dependent; what remains constant is the directional nature of the signal processed; neurons endowed with this spatial field are a major class (70%) of cells of the parietal network; within the global tuning field of parietal neurons, hand-related signals are probably 'imposed' and emerge thanks to the cortico-cortical projections from premotor cortex, as well as visual and eye information in premotor cell activity might critically depend on the parietal input.

Thus, the parieto-occipital lesion impairs not only the parietal cortical operations, but also the interplay between parietal and frontal cortex, due to degeneration of their reciprocal association systems. In such a way, the early mechanisms of the combination of different signals within the global tuning field of parietal neurons becomes impossible and the basis for the interplay between parietal and frontal cortex is disrupted. The symptoms are task dependent, since what is lost within the network are only certain combinations of signals, not the single signals *per se*.

In conclusion, optic ataxia can be regarded as the result of the breakdown of the early and context-dependent combination of eye and hand signals within the global tuning field of parietal neurons. In normal condition, the result of this combination will be available to and refined by frontal cortex. Within this network there is no serial, but only parallel processing of signals. The role of different cortical areas probably depends on where they are located within the gradient architecture of the network, and therefore which signals they predominantly, not exclusively, process. This is compatible with a planning of reaching either in eye (Lacquaniti *et al.*, 1995; McIntyre *et al.*, 1997, 1998; Batista *et al.*, 1999) or in limb (Lacquaniti *et al.*, 1995) coordinates, depending on the behavioral task. Hierarchy between parietal and frontal cortex may be dependent on the absence in the former, and presence in the latter, of the access to the peripheral motor apparatus of the spinal cord.

Notes

We are very grateful to Milena Raffi for her contribution to an early phase of part of this research and to Apostolos P. Georgopoulos for the many useful suggestions concerning quantitative data analysis. The Human Frontier Science Program, the MURST and the Ministry of Health of Italy supported this work.

Address correspondence to Roberto Caminiti, Dipartimento di Fisiologia umana e Farmacologia, Università di Roma 'la Sapienza', piazzale Aldo Moro 5, 00185 Rome, Italy. Email: roberto.caminiti@uniroma1.it.

List of abbreviations

AP	antero-posterior
CS	central sulcus
D1	eye reaction time in the IDR task
D2	eye movement time in the IDR task
D3	part of instructed delay-time in the IDR task
F2	caudal part of dorsal premotor area; PMdc, area 6aα (part)
F2 pa	peri-arcuate zone of F2; area 6aα (part)
F2 pre-CD	area F2 around the pre-central dimple; area 6aα (part)
F7	rostral part of dorsal premotor area; PMdr, area 6aβ (part)
FOE	focus of expansion
FP	fixation point
IDR	Instructed-Delay Reach task
IDR-d	Instructed-Delay Reach task in total darkness
IDR-l	Instructed-Delay Reach task in normal light conditions
IDT	instructed-delay time
IPS	intraparietal sulcus
MIP	medial intraparietal area; area 5 (part)
ML	medio-lateral
MT	movement time
PEa	parietal area PEa; area 5 (part)
PEc	parietal area PEc; area 5 (part)
POM	medial parieto-occipital sulcus
POS	parieto-occipital sulcus
R	Reach task
RF	Reach-Fixation task
RMT	reaction and movement time
RT	reaction time
S	Saccade task
SPL	superior parietal lobule
STS	superior temporal sulcus
THT	target-holding time
V1	striate cortex
V6A	visual area 6A, area 19 (part)
VF	Visual Fixation task

References

Balint R (1909) Seelenlähmung des 'schauens', optische ataxie, räumliche störung der aufmerksamkeit. Monogr Psychiatr Neurol 25:5–81.

Batschelet L (1981) Circular statistics in biology. New York: Academic Press.

Batista AP, Buneo CA, Snyder LH, Andersen RA (1999) Reach plans in eye-centered coordinates. Science 285:257–260.

Battaglia-Mayer A, Ferraina S, Marconi B, Bullis JB, Lacquaniti F, Burnod Y, Baraduc P, Caminiti R (1998) Early motor influences on visuomotor transformations for reaching. A positive image of optic ataxia. Exp Brain Res 123:172–189.

Battaglia-Mayer A, Ferraina S, Mitsuda T, Marconi B, Genovesio A, Onorati P, Lacquaniti F, Caminiti R (2000) Early coding of reaching in the parieto-occipital cortex. J Neurophysiol 83:2374–2391.

Burnod Y, Grandguillaume P, Otto I, Ferraina S, Johnson PB, Caminiti R (1992) Model of visuo-motor transformations performed by the cerebral cortex to command arm movements at visual targets in 3-D space. J Neurosci 12:1435–1453.

Burnod Y, Baraduc P, Battaglia-Mayer A, Guigon E, Koechlin E, Ferraina S, Lacquaniti F, Caminiti R (1999) Parieto-frontal coding of reaching: an integrated framework. Exp Brain Res 129:325–346.

Caminiti R, Johnson PB, Galli C, Ferraina S, Burnod Y (1991) Making arm movements within different parts of space: the premotor and motor cortical representation of a coordinate system for reaching to visual targets. J Neurosci 11:1182–1197.

Caminiti R, Ferraina S, Johnson PB (1996) The source of visual information to the primate frontal lobe: a novel role for the superior parietal lobule. Cereb Cortex 6:319–328.

Caminiti R, Ferraina S, Battaglia-Mayer A (1998) Visuomotor transformations: early cortical mechanisms of reaching. Curr Opin Neurobiol 8:753–761.

Caminiti R, Genovesio A, Marconi B, Battaglia-Mayer A, Onorati P, Ferraina S, Mitsuda T, Giannetti S, Squatrito S, Maioli MG, Molinari M (1999) Early coding of reaching: frontal and parietal association connections of parieto-occipital cortex. Eur J Neurosci 11:3339–3345.

Critchley MD (1953) The parietal lobe. New York: Hafner Press.

De Renzi E (1982) Disorders of space exploration and cognition. Chichester: Wiley.

Dum RP, Strick PL (1991) The origin of corticospinal projections from the premotor areas in the frontal lobe. J Neurosci 11:667–689.

Edelman, GM (1993) Neural Darwinism: selection and reentrant signaling in higher brain functions. Neuron 10:115–125.

Ferraina S, Garasto MR, Battaglia-Mayer A, Ferraresi P, Johnson PB, Lacquaniti F, Caminiti R (1997a) Visual control of hand reaching movement: activity in parietal area 7m. Eur J Neurosci 9:1090–1095.

Ferraina S, Johnson PB, Garasto MR, Battaglia-Mayer A, Ercolani L, Bianchi L, Lacquaniti F, Caminiti R (1997b) Combination of hand and gaze signals during reaching: activity in parietal area 7m in the monkey. J Neurophysiol 77:1034–1038.

Ferraina S, Battaglia-Mayer A, Genovesio A, Marconi B, Onorati P, Caminiti R (2001) Early coding of visuomanual coordination during reaching in parietal area PEc. J Neurophysiol 85:462–467.

Fujii N, Mushiake H, Tanji J (2000) Rostrocaudal distinction of the dorsal premotor area based on oculomotor involvement. J Neurophysiol 83:1764–1769.

Galletti C, Fattori P, Kutz DF, Battaglini PP (1997) Arm movement-related neurons in the visual area V6A of the macaque superior parietal lobule. Eur J Neurosci 9:410–413.

Harvey M, Milner DA (1995) Balint's patient. Cogn Neuropsychol 12:261–281.

Head H, Holmes G (1911–1912) Sensory disturbances from cerebral lesions. Brain 34:102–254.

Johnson PB, Angelucci A, Ziparo RM, Minciacchi D, Bentivoglio M, Caminiti R (1989) Segregation and overlap of callosal and association neurons in frontal and parietal cortices of primates: a spectral and coherency analysis. J Neurosci 9:2313–2326.

Johnson PB, Ferraina S, Caminiti R (1993) Cortical networks for visual reaching. Exp Brain Res 97:361–365.

Johnson PB, Ferraina S, Bianchi L, Caminiti R (1996) Cortical networks for visual reaching: physiological and anatomical organization of frontal and parietal lobe arm regions. Cereb Cortex 6:102–119.

Johnson PB, Ferraina S, Garasto MR, Battaglia-Mayer A, Ercolani L, Burnod Y, Caminiti R (1997) From vision to movement: cortico-cortical connections and combinatorial properties of reaching-related neurons in parietal areas V6 and V6A. In: Parietal lobe contributions to orientation in 3D space (Thier P and Karnath O, eds), Exp Brain Res (Suppl) 25:221–236.

Jouffrais C, Boussaoud D (1999) Neural activity related to eye–hand coordination in the primate premotor cortex. Exp Brain Res 128:205–209.

Kalaska JF (1996) Parietal cortex area 5 and visuomotor behavior. Can J Physiol Pharmacol 74:483–498.

Lacquaniti F, Guigon E, Bianchi L, Ferraina S, Caminiti R (1995) Representing spatial information for limb movement: the role of area 5 in the monkey. Cereb Cortex 5:391–409.

Marconi B, Genovesio A, Battaglia-Mayer A, Ferraina S, Squatrito S, Molinari M, Lacquaniti F, Caminiti R (2001) Eye–hand coordination during reaching. I. Anatomical relationships between parietal and frontal cortex. Cereb Cortex 11:513–527.

McIntyre J, Stratta F, Lacquaniti F (1997) Viewer-centered frame of reference for pointing to memorized targets in three-dimensional space. J Neurophysiol 78:1601–1618.

McIntyre J, Stratta F, Lacquaniti F (1998) Short-term memory for reaching to visual targets: psychophysical evidence for body-centered reference frames. J Neurosci 18:8423–8435.

Motter BC, Mountcastle VB (1981) The functional properties of light-sensitive neurons of the posterior parietal cortex studied in waking monkeys: foveal sparing and opponent vector organization. J Neurosci 1:3–26.

Mountcastle VB (1995) The parietal system and some higher brain functions. Cereb Cortex 5:377–390.

Neggers SFW, Bakkering H (2000) Ocular gaze is anchored to the target of an ongoing pointing movement. J Neurophysiol 83:639–651.

Perenin MT, Vighetto A (1988) Optic ataxia: a specific disruption in visuomotor mechanisms. I. Different aspects of the deficit in reaching for objects. Brain 111:643–674.

Squatrito S, Raffi M, Maioli MG, Battaglia-Mayer A (2001) Visual motion responses of neurons in the caudal area PE of macaque monkey. J Neurosci 21:RC130 (1–5).

Trevarthen CB (1968) Two mechanisms of vision in primates. Psychol Forschung 31:229–337.

Wise SP, Boussaoud D, Johnson PB, Caminiti R (1997) Premotor and parietal cortex: cortico-cortical connectivity and combinatorial computations. Ann Rev Neurosci 20:25–42.